

Xenografts of primary human gynecological tumors grown under the renal capsule of NOD/SCID mice show genetic stability during serial transplantation and respond to cytotoxic chemotherapy

Joshua Z. Press^a, Jennifer A. Kenyon^a, Hui Xue^c, Melinda A. Miller^b, Alessandro De Luca^b, Dianne M. Miller^a, David G. Huntsman^b, C. Blake Gilks^b, Jessica N. McAlpine^{a,*}, Y.Z. Wang^c

^a Department of Obstetrics and Gynaecology, University of British Columbia, Vancouver, B.C., Canada V6H 3V5

^b Department of Pathology, Genetic Pathology Evaluation Centre, Vancouver General Hospital, Centre for Translation and Applied Genomics, BC Cancer Agency and University of British Columbia, Vancouver, BC, Canada V5Z 4E6

^c Department of Cancer Endocrinology, BC Cancer Agency, Vancouver, BC, Canada V5Z 4E6

Received 12 December 2007

Available online 10 June 2008

Abstract

Objectives. Human cancer tissue xenograft models may provide a more accurate reflection of tumor biology than cell lines. This study evaluates the genetic and phenotypic stability of primary human gynecological tumors grown as serially transplanted xenografts. The response to conventional chemotherapy and novel molecular targeted chemotherapy is assessed in one of the transplantable xenograft lines.

Methods. Fresh tumor was transplanted beneath the renal capsule of NOD/SCID mice. Transplantable tumor lines were derived from 5 tumors (4 ovarian carcinomas and 1 uterine sarcoma), and serially transplanted for 2–6 generations. Comparisons were made between primary tumor and corresponding transplantable xenografts by CGH array, immunohistochemistry, and BRCA mutation analysis. Transplantable xenografts created from known BRCA1 germline mutation carriers were analyzed for histopathologic response (tumor volume, apoptotic and mitotic indices) to combination carboplatin/paclitaxel and to PARP inhibitor (PJ34).

Results. Unsupervised hierarchical cluster analysis applied to a 287 feature CGH array demonstrated a low degree of intratumoral genetic variation in 4/5 cases, with greater degree of variation in the fifth case (clear cell ovarian carcinoma derived from an omental sample). Assessment of proliferation using MIB-1 staining was concordant between primary tumor and transplantable xenograft in all ovarian cancer cases. BRCA mutation analysis identified germline BRCA1 mutation for further testing and this xenograft showed a significant response to carboplatin/paclitaxel chemotherapy, including a decrease in tumor volume and proliferation but did not demonstrate a response to the poly (ADP-ribose) polymerase-1 inhibitor PJ34.

Conclusions. Xenografts derived from gynecologic tumors can be serially transplanted and grown under renal capsule of NOD/SCID mice with minimal genetic change. This model may be used to study progression of tumors, identify therapeutic targets, and test treatment modalities in tumors with well-characterized abnormalities in genes of fundamental importance in ovarian carcinogenesis, such as loss of BRCA1.

© 2008 Elsevier Inc. All rights reserved.

Keywords: Ovarian carcinoma; Xenograft mouse model; BRCA genes; Chemotherapy; PARP inhibitor

Introduction

Despite more aggressive surgery and the development of new therapeutic modalities, successful treatment outcomes for patients with ovarian carcinoma or uterine sarcoma have been limited by late detection, with advanced stage disease at presentation, and the frequent development of chemoresistance

* Corresponding author. Department of Gynecology and Obstetrics, Division of Gynecologic Oncology, University of British Columbia, 2775 Laurel St, 6th Floor, Vancouver, BC, Canada V5Z-1M9. Fax: +1 604 875 4869.

E-mail address: jessica.mcalpine@vch.ca (J.N. McAlpine).

[1,2]. The creation of models which accurately reflect the genetic and phenotypic features of primary tumors, and their response to treatment, is an important step in identifying novel therapeutic targets and testing new treatment modalities [3]. The limited availability of animal models that spontaneously develop ovarian tumors comparable to human ovarian carcinoma has necessitated the use of *in vitro* studies with cancer cell lines and primary cultures. The creation of these renewable tumor cell lines requires tumor cells to be immortalized and then propagated within the environment of *in vitro* culture systems. It is possible to create xenograft models by implanting these lines of *in vitro* propagated cells into immunodeficient mice; however, the inconsistent response to therapeutic agents suggest that these models do not adequately reflect the human tumors *in vivo* [4]. For example, although the anti-angiogenic drug endostatin exhibited strong anti-tumor properties against *in vitro* propagated cell lines grown subcutaneously in syngeneic mice, they showed no activity in human Phase I trials [5,6]. Recently there have been several genetically engineered mouse models that develop ovarian carcinoma, providing insight into stepwise molecular progression that can lead to cancer [7]. However, it remains to be seen whether these models will adequately represent human tumors in terms of their response to treatment.

Human cancer tissue xenograft models may also be established by obtaining tumor tissue directly from the operating room at the time of primary debulking surgery, and then implanting this fresh, histologically intact tumor tissue into immunodeficient mice. Previously, we were able to show consistently high engraftment rates of ovarian cancer xenografts derived by introducing viable human tumor tissue into the subrenal compartment of NOD/SCID mice [8]. Histological examination of these tumors demonstrated preservation of immunophenotype and morphology. It has subsequently proven possible to serially transplant the tumor tissue growing within the subrenal compartment of these mice into new NOD/SCID mice. The maintenance of genetic and phenotypic stability within these transplantable tumor lines is fundamental to ensure that this model adequately represents the underlying genetic changes of primary gynecological malignancies, and has not diverged from the primary tumor with serial transplantation. Therefore, we performed a comparative analysis between primary human gynecological tumors and their corresponding serially transplanted xenografts to assess genetic and phenotypic stability. One of these transplantable xenograft lines was derived from primary tumor tissue which was surgically excised from a woman known to have a germline BRCA1 mutation. This provides a model for testing novel targeted therapy such as inhibitors of poly(ADP-ribose) polymerase-1 (PARP-1), which target defects in DNA repair in BRCA-null tumor cells. Specifically, in normal cells, single-stranded (SS) DNA breaks activate PARP-1, which facilitates DNA repair via base-excision repair pathway. If SS DNA breaks are not repaired, they become double strand breaks during mitosis. BRCA1 (and 2) are involved in the repair of DS breaks via the homologous recombination (HR) pathway. Inhibition of PARP-1 leads to less effective SS break repair and an increase in DS breaks. Cells that do not express BRCA1 (or 2) will be unable to repair their

DNA (or will have error prone repair) with resulting cell death [9,10]. This treatment strategy is particularly attractive as it targets an abnormality in tumor cells but should not impact normal cells.

Materials and methods

Tumor tissue samples

The human tumor specimens were obtained with informed consent from patients undergoing surgery at Vancouver General Hospital following a protocol approved by the University of British Columbia Clinical Research Ethics Board. Fresh tumor tissue was used to develop xenografts, a portion was snap frozen at -80°C , and some tumor tissue was fixed in 10% neutral buffered formalin and paraffin embedded.

Grafting procedure

Subrenal capsule grafting procedure was performed as described previously [9]. Briefly, under sterile conditions, a skin incision of approximately 2 cm was made along the dorsal midline of an anesthetized female mouse. An incision was then made in the body wall slightly shorter than the long axis of the kidney. The kidney was slipped out of the body cavity by applying pressure on the other side of the organ using a forefinger and thumb. After exteriorization of the kidney, #5 fine forceps were used to gently pinch and lift the capsule from the renal parenchyma to allow a 2–4 mm incision in the capsule using fine spring-loaded scissors. A pocket between the kidney capsule and the parenchyma was then created by blunt dissection. Care was taken not to damage the parenchyma and thus prevent bleeding. The graft was transferred to the surface of the kidney using blunt-ended forceps. The cut edge of the renal capsule was lifted with fine forceps, and the graft inserted into the pocket under the capsule using a fire-polished glass pipette. Two or three grafts per kidney could be placed under the renal capsule. The kidney was then gently eased back into the body cavity and the body wall and skin incisions sutured. Mice were housed in groups of three in micro-isolators with free access to food and water and their health was monitored daily. Animal care and experiments were carried out in accordance with the guidelines of the Canadian Council on Animal Care. After 60 days of growth (or earlier if required by the health status of the hosts) the animals were sacrificed in a CO_2 chamber for necropsy. Tumors were harvested, measured, photographed and fixed for histopathological analysis. Some of the rapidly growing tumors were selected for serial subrenal capsule transplantation into female NOD/SCID mice for multiple generations. Five transplantable lines, from five donors, were developed and used in this study.

Tissue microarray construction

Hematoxylin and eosin (H and E) stained sections of the primary tumour, the initial xenograft, and the most recent transplant xenograft (ie. highest passage number) were reviewed and representative areas of tumor were selected and marked. Corresponding areas on the paraffin blocks were marked, and using a Tissue Microarrayer (Beecher Instruments, Silver Spring, MD) three

Table 1
Characteristics of tumors

| Case # | Histopathology of primary tumor | Grade | Origin of xenograft | Generation of xenotransplant* |
|--------|---------------------------------|-------|---------------------|-------------------------------|
| 1 | Papillary serous carcinoma | 3 | Ovary | 6 |
| 2 | Leiomyosarcoma | High | Uterus | 3 |
| 3 | Papillary serous carcinoma | 3 | Ovary | 2 |
| 4 | Papillary serous carcinoma | 3 | Ovary | 2 |
| 5 | Clear cell carcinoma | 3 | Omentum | 4 |

*Generation of xenotransplant refers to the number of generations of serially transplanted xenografts created from the primary tumor.

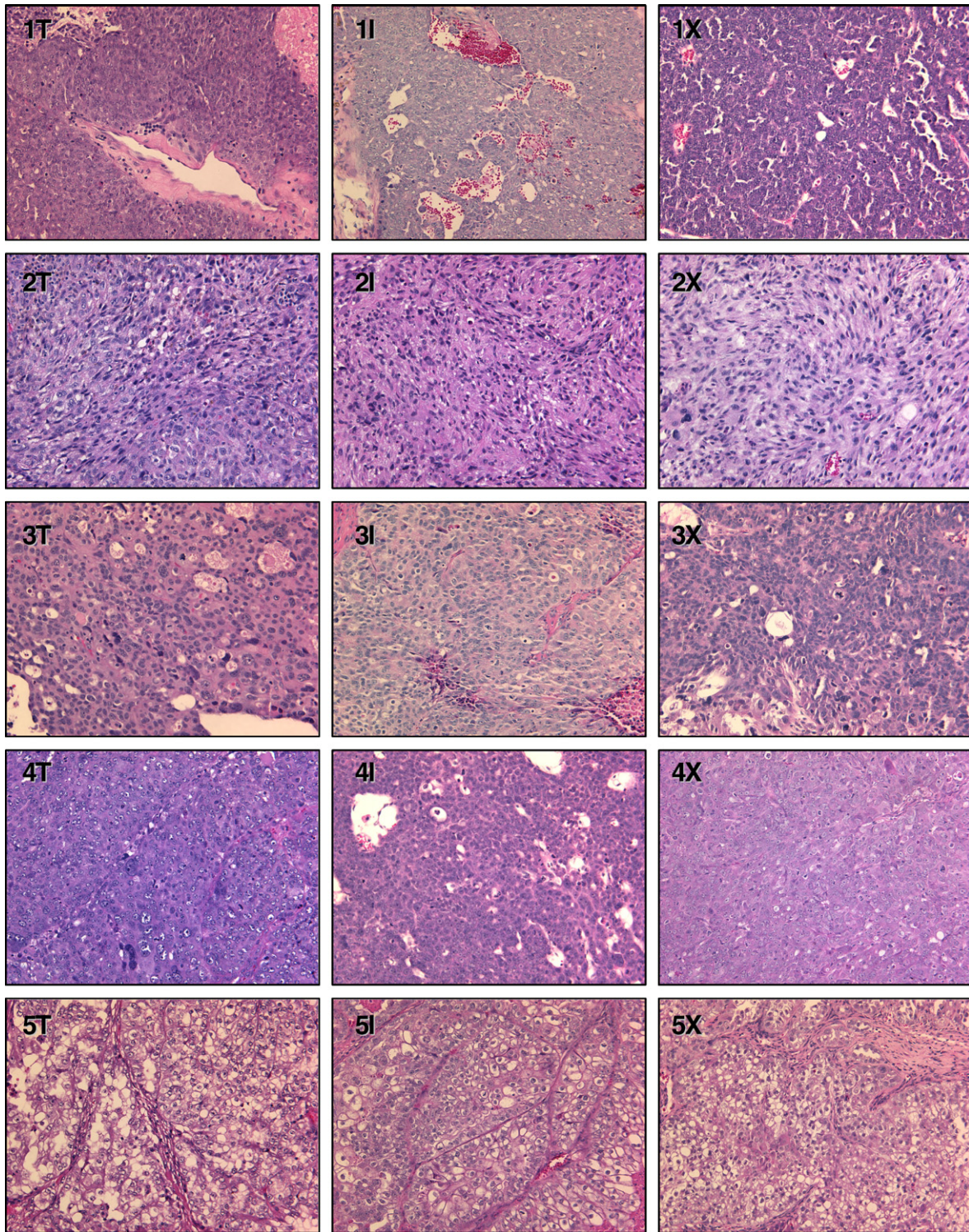


Fig. 1. Histopathology of primary tumors with corresponding initial xenograft and transplantable xenograft. 1–5 refers to case number. T = primary tumor tissue, I = initial xenograft tissue, X = transplantable xenograft line tissue.

tissue cores from the representative areas in the donor blocks were removed with a 0.6 mm diameter needle and inserted into a single recipient paraffin block. Sections were cut from the tissue microarray (TMA) block using a standard microtome. These TMA sections therefore included triplicate cores from each donor, initial xenograft and the most recent (highest generation) serially transplanted xenograft.

Immunohistochemical staining and tissue microarray analysis

TMA sections were cut at a thickness of 4 μm and mounted on glass microscope slides. Sections were dewaxed in HistoClear and hydrated in graded alcohol solutions and distilled water. H&E staining was performed to ensure adequate representation of the tumors on the TMA. Each TMA underwent

Table 2
MIB-1 proliferative indices of primary tumor, initial xenograft and transplantable tumor line

| Case # | Primary tumor* | Initial xenograft* | Tranplantable xenograft* |
|--------|----------------|--------------------|--------------------------|
| 1 | 43 | 36 | 39 |
| 2 | 25 | 30 | 39 |
| 3 | 33 | 32 | 38 |
| 4 | 41 | 44 | 44 |
| 5 | 18 | 23 | 21 |

*Percent of positively stained tumor cell nuclei.

immunohistochemical staining for MIB-1 and the number of positively staining nuclei per 50 tumor cells in a randomly selected field was counted from each of 2 cores (multiple sites assessed for each core) and averaged (BG).

Array comparative genomic hybridization (CGH)

Genetic stability of the transplantable tumor xenograft model was verified with array CGH, using the GenoSensor array system which includes 287 loci known to play an important role in oncogenesis. H and E slides from tumor samples taken facing the snap-frozen samples were reviewed to ensure that samples consisted of >70% tumor cell nuclei. DNA was extracted using the Genra DNA extraction kit (Genra Systems, Minneapolis, MN). DNA was extracted from three separate pieces of the primary tumor tissue sample. In brief, frozen tumor tissue was digested in cell lysis solution, treated with Proteinase K solution and RNase A solution, and precipitated with protein precipitation solution. DNA was suspended in DNA Hydration solution (Genra Systems, Minneapolis, MN), and the concentration was determined spectrophotometrically. Array CGH was performed using the GenoSensor Array 300 Assay (Vysis, Des Plaines, IL). Random primer mix was used to label 100 ng of tumor DNA with Cy3, and 100 ng normal male human reference DNA was labeled with Cy5. Products were purified with Amersham MicroSpin columns (Amersham, Piscataway, NJ), precipitated with 3 M sodium acetate and 100% ethanol, and resuspended in Tris (pH 8.0). Probe quality was checked by running the products on a 2% agarose gel prior to combining the test and reference probes. The probe mix was applied to GenoSensor microarrays and hybridized for 72 h at 37 °C. Microarrays were washed in 1× SSC/0.1% NP-40 at 58 °C for 5 min, 0.1× SSC/0.1% NP-40 at 58 °C for 4 min, and then 1× SSC for 1 min. Microarrays were then rinsed in ddH₂O and covered with DAPI mounting solution. Imaging and data analysis of the arrays was done with the GenoSensor Reader System (Vysis, Des Plaines, IL). The software automatically captured images of each chip, specific for the blue, the green, and the red color planes. The test/reference ratio was defined as the ratio of the sum of test intensity pixel values to the sum of reference intensity pixel values, after pixel intensity analysis within each individual spot and local background subtraction. Data was converted into a Microsoft Excel file, and BRB Array Tools [11] was used for unsupervised hierarchical clustering to create a dendrogram. In addition, the total number of genes demonstrating copy number gains or deletions was tabulated for each tumor and xenograft sample. The frequency of gain or deletion was then compared between the 3 primary tumor samples and the corresponding xenograft using the Signed-Rank Test or Wilcoxon Test. Statistical Analysis of Microarrays (SAM) was used to identify any genes showing significant differences in copy number in the primary tumors compared to the transplantable xenografts [12].

Analysis of BRCA1 and BRCA2

Polymerase chain reactions of BRCA1 exon 2 and BRCA2 exon 3 were performed in 25- μ l final volume containing 2.5 μ l of 10x PCR buffer with 10 mM of MgSO₄ (Roche Diagnostics Mannheim, Germany), 200 μ M dNTPs, 0.6 μ M primers, 50 ng tumor DNA, and 0.5 U Pwo enzyme (Roche Diagnostics, Mannheim, Germany). Primers used were BRCA1 exon 2 (forward 5'-atgaagtgtcattttataaacctttt-3', reverse primer 5'-cacaagagtgtattaattgggattc-3') and BRCA2 exon 3 (forward 5'-cccgcgccccgcctgccttaacaaaagtaacatagtc-3', reverse 5'-gcaaatcagctctctggccgcg-3'). The same touchdown protocol was

used to amplify BRCA1 exon 2 and BRCA2 exon 3. Initial denaturation at 95 °C for 2 min was followed by 14 cycles of denaturation at 95 °C for 30 s, 1 min of annealing (each cycle the annealing temperature was decreased starting from 62 °C to 55 °C in 0.5 °C increments), and extension at 72 °C for 1 min. Subsequently, 20 cycles of denaturation at 95 °C for 30 s, annealing at 55 °C for 30 s, and extension at 72 °C for 1 min were performed, followed by a final extension step at 72 °C for 7 min. PCR products were gel purified using Qiagen gel purification kit (Qiagen, Mississauga, ON), and bi-directional sequencing was performed using ABI BigDye terminator Sequencing Kit v.1.1 (Applied Biosystems, Foster City, CA) and an ABI Prism 3100 Genetic Analyzer (Applied Biosystems, Foster City, CA). Methylation of the BRCA1 promoter was assessed using methylation-specific PCR[13], and loss of heterozygosity (LOH) was analyzed using microsatellite markers[14].

Response to carboplatin/paclitaxel and poly (ADP-ribose) polymerase-1 (PARP-1) inhibitor in the transplantable tumor line with BRCA1 germline mutation

Mice carrying xenografts with the germline BRCA1 truncating mutation (del185AG) were used to test for response to conventional chemotherapy and the PARP-1 inhibitor PJ34. Four fragments of tissue (2 per kidney) were implanted for each xenografts. The control mice ($n=20$) were subjected to intraperitoneal saline injection once per week, while the experimental mice were subjected to combination intraperitoneal chemotherapy ($n=11$) with carboplatin (80 mg/kg) and paclitaxel (24 mg/kg) once weekly or PARP inhibitor PJ34 ($n=20$) at a dose of 10 mg/kg given orally twice daily. The mice were sacrificed on day 16, and tumor volume was measured prior to harvesting formalin fixed

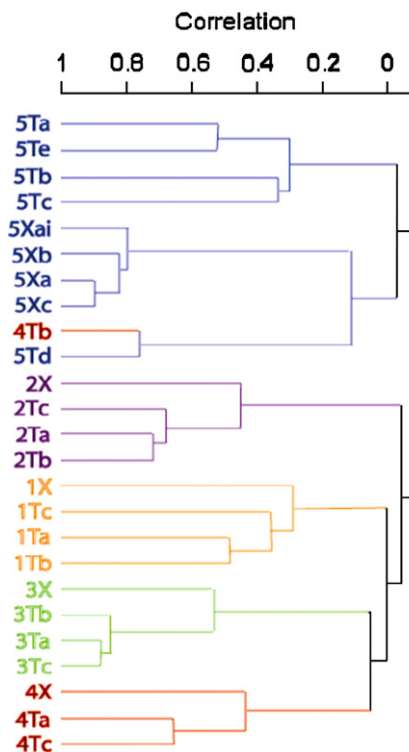


Fig. 2. Hierarchical clustering of array comparative genomic hybridization (CGH) data based on 287 loci using centered correlation and average linkage. Explanation of tumor coding system: Numbers 1–5 refers to case number, and T = primary tumor DNA, X = transplantable xenograft DNA. a–c indicates independent sampling from the different areas of the same tumor. Case 5 primary tumor samples a, b, c are from the omentum and samples d and e are from the ovary. Sample 5Xai is a replicate analysis of 5Xa. The length of the each horizontal dendrogram arm indicates the degree of correlation between the different specimens, which vary from 0% to 100% correlation. The shorter the dendrogram arm, the greater the degree of correlation.

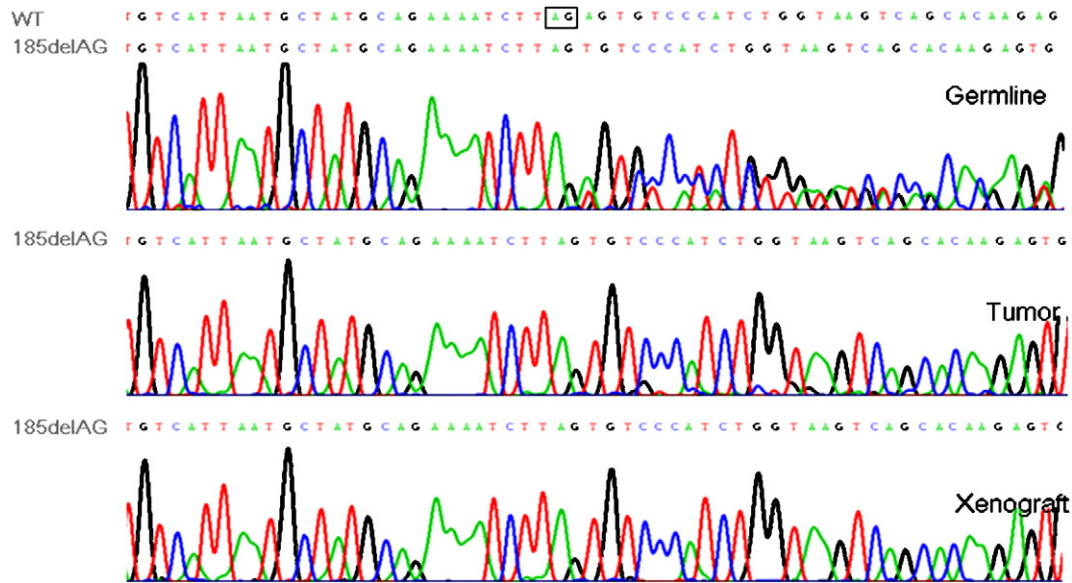


Fig. 3. Sequencing of BRCA1 exon 2 from case 4 using germline DNA, primary tumor DNA, and xenograft DNA demonstrating a 185delAG mutation in all 3 DNA samples. The normal sequence is TCTTAGAGTGTCCC. The germline demonstrates a heterozygous frameshift mutation (185delAG) resulting from deletion of an AG dinucleotide. In the wild-type allele, the AG corresponding to the deletion is evidenced by a square. In both the primary tumor and the transplantable xenograft, loss of heterozygosity (LOH) has resulted in the presence of only the mutated allele in the sequence.

paraffin embedded, OCT embedded and snap-frozen tissues. H&E stained sections were evaluated for mitotic figures and apoptotic bodies, and counts were obtained based on analysis of 50 high power microscopic fields. Data analysis was done utilizing the Tukey–Kramer means comparison test. Immunohistochemical staining for intracellular accumulation of poly (ADP-ribose) was used as a measure of inhibition of PARP-1 activity.

Results

Cases

The histopathologic and clinical characteristics of the five selected tumors (4 ovarian carcinomas and 1 uterine sarcoma) are shown in Table 1. Briefly, cases 1, 2 and 4 were high grade serous carcinomas of the ovary, case 3 was a high grade uterine sarcoma, and case 5 was a clear cell carcinoma of the ovary. A range of two to six generations of serially transplanted xenografts were created from the primary tumor.

Histopathology

Histopathologic assessment was performed with the primary tumor, initial xenograft, and the most recent transplant (highest generation). No significant differences were observed among the three tissue types with regard to cellular morphology and architecture (Fig. 1).

Immunohistochemistry

Assessment of tumor proliferation using MIB-1 staining is shown in Table 2, and the only tumor showing an increase in MIB-1 staining between primary tumor and transplantable xenograft was the uterine leiomyosarcoma (Case 2). The clear

cell ovarian carcinoma (Case 5) exhibited a lower MIB-1 index than the papillary serous ovarian carcinomas, and this was maintained in the transplantable xenograft. Analysis of the four ovarian cancers revealed no differences between primary tumor and initial xenograft ($p=0.68$), primary tumor and transplantable xenograft ($p=0.22$), nor initial xenograft and transplantable xenograft ($p=0.18$).

Array CGH

The dendrogram created from the GenoSensor array data showed similar gene copy number changes in the primary tumors and tissue from the corresponding transplantable xenograft lines (Fig. 2). There was some intratumoral variability between samples from different areas of the primary tumor, however, the primary tumor samples consistently clustered with the corresponding transplantable xenograft. Case 5 was unique as the transplantable xenograft (5X) was derived from an omental metastasis rather than the primary ovarian tumor. Three consecutive generations of case 5 transplantable xenograft tissue clustered together (5Xa-c), with the primary ovarian tumor and omental metastasis from case 5 on a separate but related branch of the dendrogram (5Ta,b,c,e). The only significant outlying sample was primary tumor from case 4b which showed closer correlation to case 5 while the other two primary tumor samples from case 4 (4Ta/4Tc) clustered with their corresponding xenograft (4X). A similar correlation between primary tumor samples and transplantable xenografts was demonstrated when K-means clustering was applied (data not shown). When the total number of loci demonstrating copy number gains or deletions were compared, there were no statistically significant differences detected between the primary tumor and corresponding xenograft

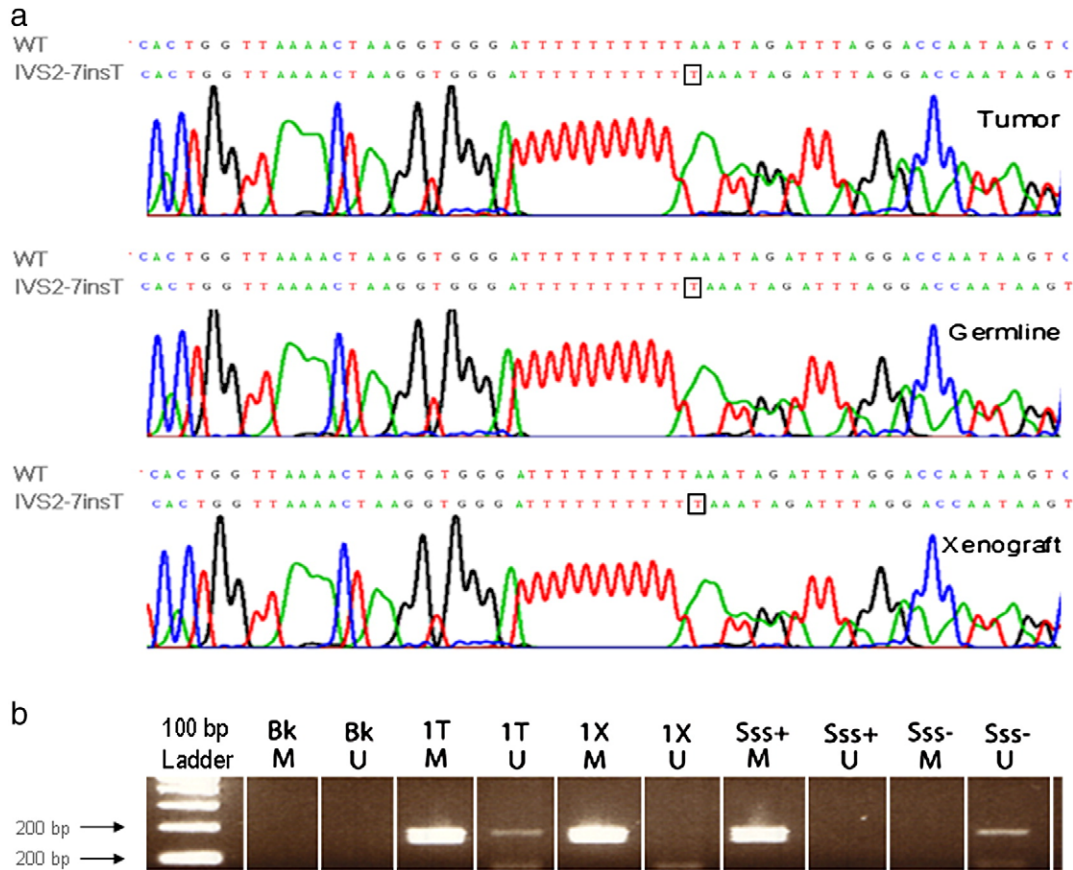


Fig. 4. (a) Sequencing of BRCA2 exon 3 from case 1 using germline DNA, primary tumor DNA, and xenograft DNA demonstrating the presence of an heterozygous IVS2-7insT unclassified variant in all 3 DNA samples. The T insertion is evidenced by a square in the mutant sequence. There is no evidence of LOH in the sequence. (b) BRCA1 promoter hypermethylation. Bk = Blank, 1T = primary tumor DNA from case 1, 1X = transplantable xenograft DNA from case 1, Sss+ = normal DNA methylated with SssI methylase, Sss- = normal DNA not treated with SssI methylase, M = PCR primers for methylated BRCA1 promoter, U = PCR primers for unmethylated BRCA1 promoter.

(data not shown). No region was significantly amplified when SAM was used to compare the transplantable xenografts with the primary tumors.

BRCA alterations

Two of the transplantable tumor lines (Case 1 and Case 4) were derived from patients with well-characterized alterations in BRCA2 and BRCA1 respectively. Sequencing of DNA extracted from the germline, primary tumor, and transplantable xenograft from case 4 demonstrated the presence of a mutation in exon 2 of BRCA1 (185delAG)[15]. In addition, the primary tumor and xenograft have lost the wild-type allele, as the sequencing product demonstrated only the presence of DNA with the 185delAG deletion (Fig. 3). LOH at the BRCA1 locus was confirmed in both case 1 and case 4, using 2 intragenic and 2 flanking microsatellite markers for BRCA1 (data not shown). Promoter hypermethylation of the BRCA1 promoter was identified in the primary tumor DNA from case 1, and this was maintained in the transplantable xenograft (Fig. 4b). There were no BRCA1 mutations in either germline or tumor DNA in case 1 (data not shown). Immunohistochemical staining with a BRCA1 antibody demonstrated loss of BRCA1 protein in both case 1 and

case 4. Sequencing of DNA from case 1 demonstrated the presence of a sequence alteration in intron 2 of BRCA2 (IVS2-7insT), which was present in DNA derived from the germline, primary tumor and transplantable xenograft (Fig. 4a). Since there was no evidence of BRCA2 LOH in the primary tumor or transplantable xenograft (data not shown), we considered IVS2-7insT an unclassified variant of BRCA2, rather than a mutation.

Tumor response to conventional chemotherapy and to PARP-1 inhibitor in a BRCA1-null transplantable xenograft

Tumor volume and mitotic index decreased significantly in the treatment group which received carboplatin/paclitaxel compared to the control group treated with only normal saline ($p < 0.0001$). There were no significant differences in apoptotic indices or mitotic indices between control mice and either the carboplatin/paclitaxel or the PARP-1 inhibitor PJ34 treatment groups (data not shown). Tumor volume was significantly less in the carboplatin/taxol treated mice compared to either the control ($p = 0.001$) or PJ34 treated animals ($p = 0.001$). There was no significant difference in tumor volume between the latter two groups ($p = 0.11$) (Fig. 5a). Immunohistochemistry demonstrated

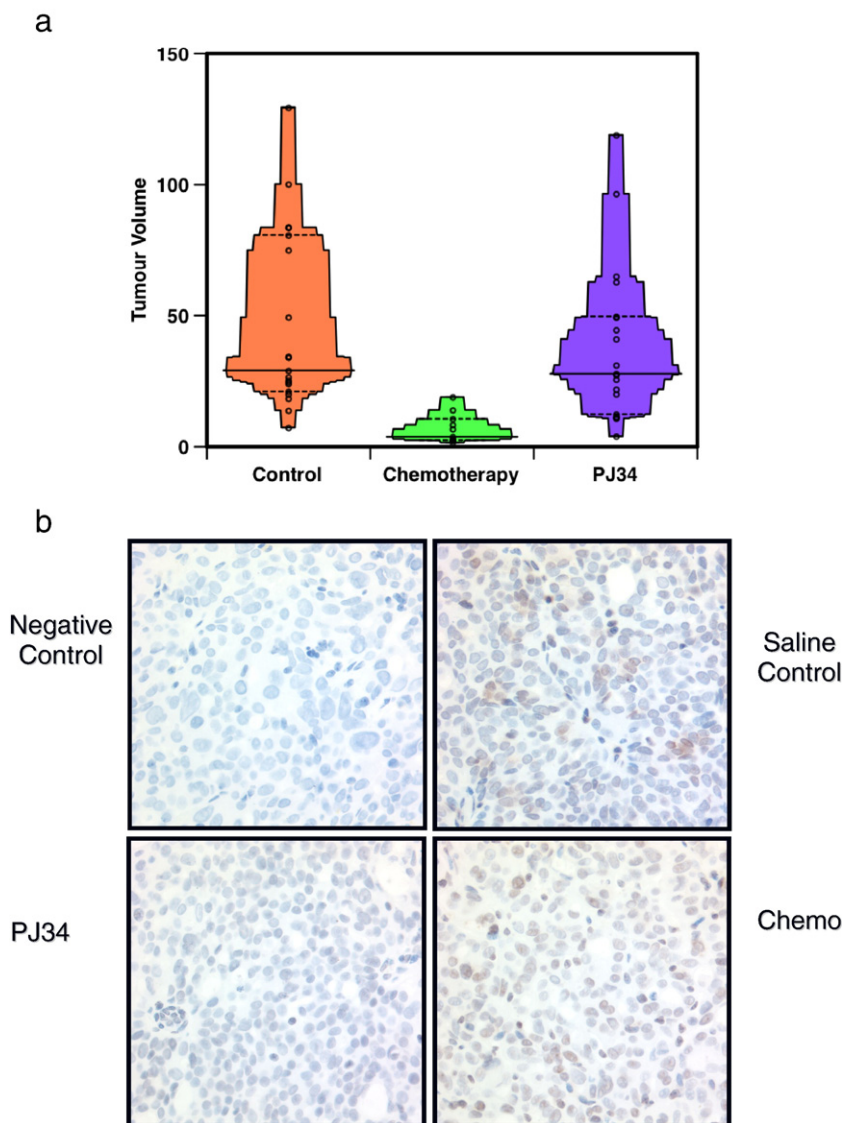


Fig. 5. (a) Tumor volume comparisons between saline control, carboplatin/paclitaxel, and the PARP-1 inhibitor PJ34 treatment group revealing a significant decrease in tumor volume in the traditional chemotherapy group. (b) Immunohistochemical staining for intracellular accumulation of poly (ADP-ribose) was used as a measure of inhibition of PARP-1 activity and demonstrates the presence of poly (ADP-ribose) in the saline control and chemotherapy treated xenografts with decreased PAR accumulation in the PJ34 treated animals.

the presence of PAR in the saline control and chemotherapy treated xenografts, with decreased (but not absent) PAR accumulation in the PJ34 treated animals (Fig. 5b).

Discussion

We previously demonstrated that the subrenal capsule site in NOD/SCID mice can be successfully used for grafting both low and high grade primary human ovarian tumors, overcoming previous problems of poor engraftment rates. We also showed morphological and biomarker stability between the primary tumor and the initial xenograft. In the current study, we have expanded on our investigations with primary xenografts, demonstrating changes (histopathologic and morphometric) following treatment with chemotherapy that are consistent with those seen in women receiving neoadjuvant chemotherapy for

ovarian carcinoma [16–18]. Further, we have demonstrated the development of transplantable tumor lines from another cohort of xenografts, with some cases achieving up to 6 successive generations. Such transplantable lines provide renewable preclinical models to test new therapeutic agents and will allow analysis of tumor progression at cellular and molecular levels. Inherent in such a model is the possibility of genetic drift and altered phenotypic characteristics of the tissue occurring during serial transplantation, thereby potentially reducing their relevance.

Our transplantable xenograft model demonstrated genetic and phenotypic concordance between primary tumor and transplantable xenograft. MIB-1 staining as an assessment of proliferation was similar between primary tumor and transplantable xenograft in all ovarian cancer cases. Array CGH data does demonstrate some minor genetic differences between the primary tumor and the corresponding transplantable xenograft; however, the degree of

genetic variation is similar to that present between tissue samples taken from different regions of the same primary tumor (i.e. intratumoral heterogeneity).

Our xenograft model derived from serially transplanting fresh tumor tissue from mouse to mouse over successive generations provides a model which is not only renewable, but also maintains genetic and phenotypic stability during serial transplantation. It also allows testing of xenografts, which have been extensively characterized, something not possible with short term primary xenograft experiments. Importantly, these tissues have been successfully cryopreserved and can be utilized in future experiments.

To establish the potential utility of our model we assessed the sensitivity of the BRCA1-null xenograft to carboplatin/paclitaxel chemotherapy and PARP inhibitors. Cells that have BRCA1 abnormalities are known to be hypersensitive to chemicals that produce double-stranded DNA breaks, including cisplatin and mitomycin C [19]. This laboratory observation correlates clinically with reports showing significantly improved survival among patients with BRCA-associated ovarian cancer, compared to sporadic cases [20]. The sensitivity of our BRCA1-null xenograft model to DNA damaging chemotherapy, as reflected by decreased tumor volume, further supports the ability of our model system to reflect primary tumor behavior. A new strategy for treatment of cancer in patients with BRCA1 and BRCA2 has been proposed based on inhibition of a protein called PARP, which is important for repairing single-strand breaks in DNA [9]. It has been suggested that inhibiting PARP should lead to the formation of DNA single-strand breaks. These single-strand breaks are then converted to double strand breaks during mitosis and these cannot be repaired accurately in cells which lack BRCA1 or BRCA2. DNA damage would in turn lead to tumor cell death [21]. This has been demonstrated using *in vitro* models where PARP inhibition resulted in much greater reduction in cell survival in BRCA1/BRCA2 deficient cells compared to wild-type cells [10]. The tumor cell models of BRCA1 and BRCA2 deficiency available at the time of these studies were not suitable for xenograft development, for the *in vivo* testing of PARP inhibitors, in contrast to the transplantable xenograft line with a BRCA1 mutation described herein. Our initial experiments did not demonstrate inhibition of tumor growth with the chosen PARP-1 inhibitor (PJ34). Although the doses of PJ34 used have previously been shown to be active in animal experiments [22–24], there was reduced but detectable PAR in this series and the lack of response may be a result of incomplete PARP-1 inhibition. New investigations with a more active PARP-1 inhibitor are underway. Given our recent appreciation of the high percentage (>35%) germline or somatic BRCA1 mutations, or epigenetic loss of BRCA1 in epithelial ovarian cancers, particularly serous carcinomas, further exploration of PARP-1 targeted therapy is particularly appealing [25].

In conclusion, in this study we have expanded on our primary xenograft investigations and demonstrated successful creation of transplantable xenograft lines derived from primary tumor tissue, which maintain genetic and biomarker stability over successive generations. This will provide researchers with a renewable resource, which may contribute to our understanding of carcinogenesis, and assist in the identification of novel therapeutic targets, facilitating development of innovative therapeutic regimens.

Conflict of interest statement

The authors have no conflicts of interest to declare.

Acknowledgments

This work was supported in part by NCI Canada grant No. 017051, and a grant from the National Ovarian Cancer Association, Canada (CBG). Supported was also provided by an unrestricted educational grant from sanofi-aventis (DGH), and from OvCaRe, an initiative of the VGH and UBC Hospital Foundation and the BC Cancer Foundation, Vancouver, Canada (YZW). Dr. David G. Huntsman is a Michael Smith Foundation for Health Research Scholar. ArrayCGH analysis was performed using BRB ArrayTools developed by Dr. Richard Simon and Amy Peng Lam.

References

- [1] Cannistra SA. Cancer of the ovary. *N Engl J Med* 2004;351:2519–29.
- [2] Giuntoli II RL, Metzinger DS, DiMarco CS, Cha SS, Sloan JA, Keeney GL, et al. Retrospective review of 208 patients with leiomyosarcoma of the uterus: prognostic indicators, surgical management, and adjuvant therapy. *Gynecol Oncol* 2003;89:460–9.
- [3] Kerbel RS. Human tumor xenografts as predictive preclinical models for anticancer drug activity in humans: better than commonly perceived-but they can be improved. *Cancer Biol Ther* 2003;2:S134–9.
- [4] Buick RN, Pullano R, Trent JM. Comparative properties of five human ovarian adenocarcinoma cell lines. *Cancer Res* 1985;45:3668–76.
- [5] Boehm T, Folkman J, Browder T, O'Reilly MS. Antiangiogenic therapy of experimental cancer does not induce acquired drug resistance. *Nature* 1997;390:404–7.
- [6] Eder Jr JP, Supko JG, Clark JW, Puchalski TA, Garcia-Carbonero R, Ryan DP, et al. Phase I clinical trial of recombinant human endostatin administered as a short intravenous infusion repeated daily. *J Clin Oncol* 2002;20: 3772–84.
- [7] Boyd J. Mouse models of gynecologic pathology. *N Engl J Med* 2005;352: 2240–2.
- [8] Lee CH, Xue H, Sutcliffe M, Gout PW, Huntsman DG, Miller DM, et al. Establishment of subrenal capsule xenografts of primary human ovarian tumors in SCID mice: potential models. *Gynecol Oncol* 2005;96: 48–55.
- [9] Bryant HE, Schultz N, Thomas HD, Parker KM, Flower D, Lopez E, et al. Specific killing of BRCA2-deficient tumours with inhibitors of poly(ADP-ribose) polymerase. *Nature* 2005;434:913–7.
- [10] Farmer H, McCabe N, Lord CJ, Tutt AN, Johnson DA, Richardson TB, et al. Targeting the DNA repair defect in BRCA mutant cells as a therapeutic strategy. *Nature* 2005;434:917–21.
- [11] Zorn KK, Bonome T, Gangi L, Chandramouli GV, Awtrey CS, Gardner GJ, et al. Gene expression profiles of serous, endometrioid, and clear cell subtypes of ovarian and endometrial cancer. *Clin Cancer Res* 2005;11:6422–30.
- [12] Tusher VG, Tibshirani R, Chu G. Significance analysis of microarrays applied to the ionizing radiation response. *Proc Natl Acad Sci U S A* 2001;98:5116–21.
- [13] Baldwin RL, Nemeth E, Tran H, Shvartsman H, Cass I, Narod S, et al. BRCA1 promoter region hypermethylation in ovarian carcinoma: a population-based study. *Cancer Res* 2000;60:5329–33.
- [14] Chan KY, Ozcelik H, Cheung AN, Ngan HY, Khoo US. Epigenetic factors controlling the BRCA1 and BRCA2 genes in sporadic ovarian cancer. *Cancer Res* 2002;62:4151–6.
- [15] Liede A, Karlan BY, Baldwin RL, Platt LD, Kuperstein G, Narod SA. Cancer incidence in a population of Jewish women at risk of ovarian cancer. *J Clin Oncol* 2002;20:1570–7.
- [16] McCluggage WG, Lyness RW, Atkinson RJ, Dobbs SP, Harley I, McClelland HR, et al. Morphological effects of chemotherapy on ovarian carcinoma. *J Clin Pathol* 2002;55:27–31.
- [17] Sassen S, Schmalfeldt B, Avril N, Kuhn W, Busch R, Hofler H, et al. Histopathologic assessment of tumor regression after neoadjuvant

- chemotherapy in advanced-stage ovarian cancer. *Hum Pathol* 2007;38:926–34.
- [18] Le T, Williams K, Senterman M, Hopkins L, Faught W, Fung-Kee-Fung M. Histopathologic assessment of chemotherapy effects in epithelial ovarian cancer patients treated with neoadjuvant chemotherapy and delayed primary surgical debulking. *Gynecol Oncol* 2007;106:160–3.
- [19] Moynahan ME, Cui TY, Jasin M. Homology-directed DNA repair, mitomycin-c resistance, and chromosome stability is restored with correction of a Brca1 mutation. *Cancer Res* 2001;61:4842–50.
- [20] Boyd J, Sonoda Y, Federici MG, Bogomolnii F, Rhei E, Maresco DL, et al. Clinicopathologic features of BRCA-linked and sporadic ovarian cancer. *Jama* 2000;283:2260–5.
- [21] Turner N, Tutt A, Ashworth A. Targeting the DNA repair defect of BRCA tumours. *Curr Opin Pharmacol* 2005;5:388–93.
- [22] Scott GS, Kean RB, Mikheeva T, Fabis MJ, Mabley JG, Szabo C, et al. The therapeutic effects of PJ34 [*N*-(6-oxo-5,6-dihydrophenanthridin-2-yl)-*N*,*N*-dimethylacetamide.HCl], a selective inhibitor of poly(ADP-ribose) polymerase, in experimental allergic encephalomyelitis are associated with immunomodulation. *J Pharmacol Exp Ther* 2004;310:1053–61.
- [23] Mabley JG, Jagtap P, Perretti M, Getting SJ, Salzman AL, Virag L, et al. Anti-inflammatory effects of a novel, potent inhibitor of poly (ADP-ribose) polymerase. *Inflamm Res* 2001;50:561–9.
- [24] Garcia Soriano F, Virag L, Jagtap P, Szabo E, Mabley JG, Liaudet L, et al. Diabetic endothelial dysfunction: the role of poly(ADP-ribose) polymerase activation. *Nature medicine* 2001;7:108–13.
- [25] Press JP, DeLuca A, Boyd N, Young S, Troussard A, Ridge Y, et al. Ovarian carcinomas with genetic and epigenetic BRCA1 loss have distinct molecular abnormalities. *BMC Cancer* 2008;8:17.